J. Phys. Chem. **1991**, *95*, 2652–2661

ground-state vibrational frequency was determined to be 68.1 cm^{-1}. This compares well with the vibrational frequency of the singlet state of dimanganese in krypton matrices (76.4 cm^{-1}) as well as that in argon matrices (approximately 59 and 68 cm^{-1} for the two different matrix sites).[10] All of the above results clearly indicate that Mn_2 is a weakly bound antiferromagnetic van der Waals dimer.

Acknowledgment. The authors thank NSERC and the Connaught Fund for financial support. M.M. thanks the Canada Council Killam Program for a research fellowship. T.L.H. and A.S.H. thank the Ontario Government for graduate research fellowships.

Registry No. Mn_2, 12596-53-1.

Photochemistry of Cycloalkene·NO_2 Collisional Pairs in a Cryogenic Matrix: Chemical Trapping of Cycloalkene Oxirane Biradical Conformers, and Comparison of Product Control for Excitation above and below the NO_2 Dissociation Threshold

Donald J. Fitzmaurice and Heinz Frei*

Chemical Biodynamics Division, Lawrence Berkeley Laboratory, University of California, Berkeley, California 94720 *(Received: June 29, 1990)*

Oxygen atom transfer from NO_2 to cyclohexene and from NO_2 to cyclopentene was induced by excitation of reactant pairs isolated in solid Ar by light in the wavelength range between 610 and 355 nm. Continuous wave dye, Ar ion, and Nd:YAG lasers were used as photolysis sources, and the chemistry was monitored by Fourier transform infrared spectroscopy. The O atom transfer path accessible at wavelengths longer than the 398-nm NO_2 dissociation limit led to cycloalkene oxide as the only final oxidation product. The reaction threshold was at 610 nm. In the case of cyclohexene + NO_2, two cyclohexyl nitrite radical diastereomers were produced concurrently with the epoxide. Infrared analysis based on ^{18}O and ^{15}N isotopic substitution, visible light induced wavelength-selective photodissociation, and matrix annealing experiments indicate that the two stereoisomers are cyclohexyl nitrite radical chair conformers with an equatorial and an axial C–O bond, respectively. Since these are transient cyclohexene oxirane biradicals chemically trapped by reaction with NO cage coproduct according to the previously established reaction mechanism, it is concluded that cyclohexene oxidation proceeds along two diastereomeric paths. In the case of the cyclopentene + NO_2 reaction only a single cyclopentyl nitrite radical stereoisomer is observed, presumably because of the very low barrier to pseudorotation of the pentyl ring. Loss of product specificity upon photolysis of cyclohexene/NO_2/Ar and cyclopentene/NO_2/Ar matrices above the NO_2 dissociation threshold with 355-nm light is evident from the appearance of two additional products aside from cycloalkene oxide, namely, cyclohexanone (cyclopentanone) and 2-cyclohexen-1-ol (2-cyclopenten-1-ol). Absorbance growth behavior of these products indicated that the ketone and epoxide originate from the same reservoir of sustained cycloalkene·NO_2 collisional pairs that reacts at visible wavelengths by large-amplitude O atom transfer, while cycloalkenol stems from dissociation of NO_2, followed by reaction of free O(^{3}P) with cycloalkene. It is proposed that large-amplitude oxygen atom transfer remains the dominant pathway for collisional cycloalkene·NO_2 pairs excited above the NO_2 dissociation threshold. Reaction by NO_2 predissociation is operative for reactant pairs with orientation or distances (including separation by Ar host atoms) that make the large-amplitude reaction inaccessible.

I. Introduction

We have recently observed product-specific oxidation of small, unfunctionalized alkenes by vibronic excitation of NO_2·alkene pairs in a cryogenic matrix with red light. Photons at these wavelengths excite NO_2 to vibronic levels that lie 25 kcal below the 398-nm dissociation threshold of this reactant. *cis*- and *trans*-2-butene + NO_2 give exclusively 2-butene oxides as final oxidation products with a high degree of stereochemical retention.[1,2] Alkenes with a terminal methylene group, such as ethylene[3] and isobutylene,[4] gave aldehyde as an additional product. No products that would result from breakup of the carbon skeleton were observed. Concurrent trapping of alkyl nitrite radicals allowed us to map the detailed reaction path of these mild oxidations. Strong evidence was obtained from product stereochemical analysis and photolysis wavelength dependence of the reaction kinetics for transfer of an O atom to the CC double bond by vibronically excited NO_2 to form a transient oxirane biradical. A fraction of these biradicals are chemically trapped by combination with concurrently produced NO cage neighbor to yield the observed alkyl nitrite radicals. Chemical trapping of transient oxirane biradicals in their nascent conformation by reaction with NO coproduct is a unique feature of vibronically induced chemistry of NO_2·alkene sustained collisional pairs in a matrix, revealing in unprecedented detail the stereochemistry of alkene oxidation paths.[5]

We have employed this method of controlled O atom transfer to cyclohexene and cyclopentene in order to explore in detail the stereochemical path of cycloalkene epoxidation. Cyclohexene·NO_2 and cyclopentene·NO_2 pairs were isolated in solid Ar at 12 K, and the photolysis wavelength dependence of the long wavelength visible light induced chemistry was investigated. The reaction was initiated by tuned continuous wave (CW) dye laser radiation, and the chemistry monitored by Fourier transform infrared spectroscopy. Photolysis at wavelengths shorter than 398 nm was also performed in order to compare the chemistry of sustained collisional pairs[6] above and below the NO_2 dissociation threshold. This comparison is of special interest with regard to product control. In principle, reactant excitation above the lowest dissociation limit permits access to dissociative surfaces of the isolated reactant, in addition to the large-amplitude motion path accessible to the NO_2·alkene sustained collisional pairs from vibronic levels

---

(1) Nakata, M.; Frei, H. *J. Am. Chem. Soc.* **1989**, *111*, 5240.
(2) Nakata, M.; Frei, H. *J. Phys. Chem.* **1989**, *93*, 7670.
(3) Nakata, M.; Shibuya, K.; Frei, H. *J. Phys. Chem.* **1990**, *94*, 8168.
(4) Nakata, M.; Frei, H. *J. Chem. Soc. Jpn.* **1989**, 1412.
(5) For a recent review of intermediates of hydrocarbon oxidation, see: Hucknall, D. J. *Chemistry of Hydrocarbon Combustion*; Chapman and Hall: London, 1985.
(6) Frei, H.; Pimentel, G. C. In *Chemistry and Physics of Matrix Isolated Species*; Andrews, L., Moskovits, M., Eds.; Elsevier: Amsterdam, 1989; p 139.

0022-3654/91/2095-2652$02.50/0

below the NO_2 dissociation limit. This may lead to free radical and atom chemistry that is not accessible from bound, nonpredissociative reactant levels. The results of these experiments are reported here.

II. Experimental Section

Matrix suspensions of cyclohexene (or cyclopentene) and NO_2 in solid Ar were prepared by slow continuous deposition as described previously.[1] Concentration ratios typically used were cycloalkene/NO_2/Ar = 2.5/1/100, 2.5/1/200, and 2.5/1/400. While for the latter concentration the reservoir of alkene·NO_2 reactant pairs is small, *interpretation of product spectra is facilitated* by virtue of the much smaller amounts of N_2O_4 species present in the matrix compared to the higher concentration.[1] Chemical reaction was monitored by infrared spectroscopy using an IBM-Bruker FT-IR Instrument Model IR-97 at 0.5-cm^{-1} resolution. For laser irradiation (Ar-ion laser pumped CW dye laser, Coherent Models Innova 90-6 and 599-01), the 12 K cooled CsI window was rotated 90° to expose the matrix to photolysis light entering the vacuum shroud of the cryostat (Air Products Displex Model CSA 202) through a quartz window. Laser power was measured before and after each irradiation period by using a Coherent Power Meter Model 210 situated directly in front of the quartz entrance window. For UV irradiation two sources were used, namely, the 351–364-nm lines of the CW Ar ion laser, or the pulsed, tripled output of a Nd:YAG laser (Quanta Ray Model DCR-2A) at 355 nm. The average output power of this pulsed source was measured with a Scientech Power Meter. Prior to photolysis of cycloalkene·NO_2 pairs, the matrix was irradiated for 2 h at 620 nm (400 mW cm^{-2}). At this wavelength only N_xO_y photoisomerization was induced, but no reaction of alkene·NO_2 pairs. This allowed us to minimize interference by spectral changes due to N_xO_y interconversion processes during subsequent photolysis of alkene·NO_2 pairs at shorter wavelengths. Visible matrix spectra were taken with a Shimadzu Model UV 2100 UV–vis spectrometer.

Cyclohexene (Aldrich, Gold Label), cyclopentene (Aldrich, 99%), cyclohexene oxide, cyclopentene oxide, cyclohexanone, cyclopentanone (all from Aldrich, 99%), and 2-cyclohexen-1-ol (American Tokyo Kasei, Inc.) were used as received. NO impurity was removed from NO_2 (Matheson, 99.5%) as described in previous work.[1] $N^{18}O_2$ was prepared by oxidizing $N^{18}O$ (Icon Services, Inc., 94.5 atom % ^{18}O) by $^{18}O_2$ (MSD Isotopes, 98.2 atom % ^{18}O) in the gas phase to give $N^{16}O_2/N^{16}O^{18}O/N^{18}O_2$ = 0.5/11/88 (by infrared). $^{15}NO_2$ (Icon Services, Inc., 99 atom % ^{15}N) was purified by LN_2 trap-to-trap distillation before use. Argon (Matheson, 99.998%) was used without further purification.

III. Results

Reactant spectra will be presented in subsection 1. Infrared spectra of products of cyclohexene and cyclopentene photooxidation by NO_2 at wavelengths below its dissociation threshold will be given in subsection 2. In subsection 3, results obtained for excitation of cyclohexene and cyclopentene·NO_2 pairs at 355 nm will be reported.

1. Reactant Spectra. As all infrared absorptions necessary to identify products lie in the range 2000–400 cm^{-1}, we will limit presentation of infrared spectral data mainly to this region. After deposition of a matrix cyclohexene/NO_2/Ar = 2.5/1/100, cyclohexene bands were observed at 1885, 1716, 1685, 1657, 1608, 1482, 1460, 1450, 1440, 1395, 1355, 1343, 1326, 1269, 1244, 1139, 1036, 995, 920, 904, 880, 812, 721, 677, and 643 cm^{-1}.[7] The two observed infrared absorptions of NO_2 were at 1609 and 749 cm^{-1}.[8] Depending on the matrix concentration, varying amounts of N_2O_4 isomers were trapped, together with traces of NO and N_2O_3. The spectra of these species and their photoisomerization behavior under irradiation with red, yellow, and blue light have been summarized in Table I of ref 1. In matrices cyclopentene/NO_2/Ar = 2.5/1/100, C_5H_8 infrared absorptions were found at 1635, 1625, 1475, 1453, 1444, 1356, 1348, 1301, 1285, 1279, 1205, 1133, 1043, 965, 906, 880, 697, 657, 643, and 624 cm^{-1}.[9] Hydrocarbon or NO_2 infrared bands in cycloalkene/NO_2/Ar matrices were unchanged compared to Ar matrices with only one reactant present. As in the case of 2-butenes + NO_2[1,2] and ethylene + NO_2[3] in solid Ar, cycloalkene and NO_2 cage neighbors do not cause frequency shifts of reactant infrared absorptions.

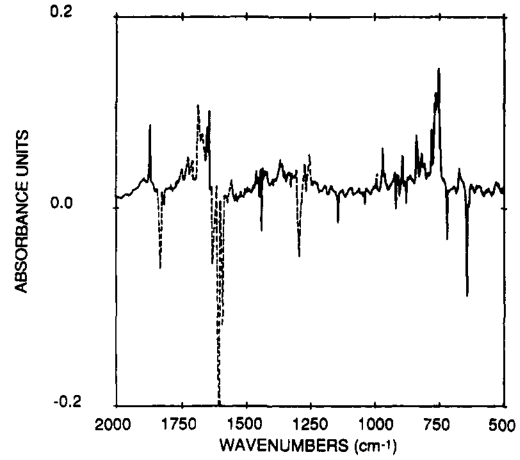

Figure 1. Infrared difference spectrum obtained upon 590-nm (600 mW cm^{-2}) irradiation of a matrix cyclohexene/NO_2/Ar = 2.5/1/100 for 10 h. Dashed lines indicate N_xO_y species.

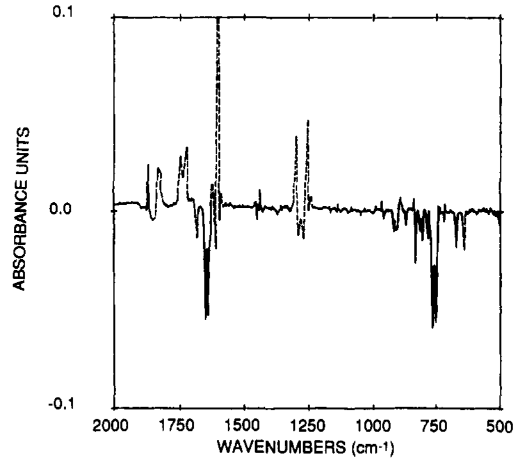

Figure 2. Infrared difference spectrum obtained upon 10-min photolysis of a matrix cyclohexene/NO_2/Ar = 2.5/1/100 by 514/488-nm Ar ion laser emission (100 mW cm^{-2}) following 10-h irradiation at 590 nm (Figure 1).

2. Photolysis below the NO_2 Dissociation Limit. (*A*) *Cyclohexene + NO_2.* While prolonged irradiation of matrices C_6H_{10}/NO_2/Ar at 620 nm and longer wavelengths resulted merely in isomerization of N_xO_y species as described earlier,[1] new infrared absorptions appeared when tuning the photolysis laser to 610 nm. Concurrently, cyclohexene and NO_2 reactant absorptions decreased. Figure 1 shows the infrared difference spectrum following 590-nm irradiation of a matrix cyclohexene/NO_2/Ar = 2.5/1/100 at 600 mW cm^{-2} for 10 h. Four product bands can readily be discerned from the spectrum even after only 30 min of photolysis, namely, at 1655, 1644, 769, and 756 cm^{-1}. A number of weaker product absorptions appeared upon prolonged 590-nm irradiation (Figure 1). The origin of these could be established by subsequent photolysis with 514- or 488-nm Ar ion laser radiation, as can be seen from Figure 2. This infrared difference spectrum displays the effect on the sample shown in Figure 1 of 10-min 514/488-nm ("all lines blue-green") irradiation (100 mW cm^{-2}). We found

---

(7) Noack, A. *Spectrochim. Acta* **1962**, *18*, 692.

(8) Fateley, W. G.; Bent, H. A.; Crawford, B., Jr. *J. Chem. Phys.* **1959**, *31*, 204.

(9) Villareal, J. R.; Laane, J.; Bush, S. F.; Harris, W. C. *Spectrochim. Acta* **1979**, *35A*, 331.

TABLE I: Infrared Spectrum Assigned to Cyclohexyl Nitrite Radical Trapped in a Cyclohexene/NO_2/Ar (2.5/1/100) Matrix

frequency cm^{-1}			depletion, abs units		
$C_6H_{10}{}^{16}ON^{16}O$	$C_6H_{10}{}^{18}ON^{18}O$	$C_6H_{10}O^{15}NO$	545 nm[a]	514/488 nm[b]	assgnt
1655	1613	1627	0.0273	0.0223	I_1
1644	1604	1616	0.0555	0.0098	I_2
1452	1452	1452	0.0031	0.0028	I_1
1430	1430	1430	0.0023	0.0009	I_2
1376	1376	1376	0.0016	0.0016	I_1
1167	1165	1165	0.0027	0.0005	I_2
1102			0.0016	0.0004	I_2
1050	1039	1049	0.0020	0.0019	I_1
1010	1010	1007	0.0020	0.0006	I_2
960	940	954	0.0050	0.0009	I_2
837	835	836	0.0094	0.0094	I_1
819	818	819	0.0086	0.0019	I_2
808	807	807	0.0062	0.0055	I_1
769	760	762	0.0266	0.0180	I_1
756	735	746	0.0469	0.0089	I_2
675	653	672	0.0074	0.0065	I_1

[a] Depletion of bands assigned to trapped cyclohexyl nitrite radical following 545-nm (150 mW cm^{-2}) irradiation of cyclohexene/NO_2/Ar (2.5/1/100) matrix at 12K for 6 h (peak absorbances). [b] Depletion of bands assigned to trapped cyclohexyl nitrite radical following 488/514-nm (100 mW cm^{-2}) irradiation of cyclohexene/NO_2/Ar (2.5/1/100) matrix at 12 K for 10 min.

that 16 bands decreased, including the 4 most prominent ones mentioned above. Frequencies of these absorptions, including those of the ^{15}N and ^{18}O counterparts obtained from analogous photolysis experiments with $^{15}NO_2$ and $N^{18}O_2$, are shown in Table I (columns 1–3).

All bands that increase upon 514/488-nm photolysis, Figure 2, are also part of the product spectrum of the 590-nm irradiation experiment. The 1872-cm^{-1} absorption, with ^{15}N and ^{18}O counterparts at 1839 and 1823 cm^{-1}, respectively, is readily assigned to NO. The other product absorptions, all listed in Table II, grow at constant relative intensities upon 590-, 514-, or 488-nm photolysis. As Table II shows, frequencies and relative intensities agree completely with an authentic infrared matrix spectrum of cyclohexene oxide (M/A = 1/200). No other product absorptions due to cyclohexene + NO_2 reaction were observed at any visible photolysis wavelength (610–458 nm).

As can be seen from Figure 2, during brief 514/488-nm photolysis, reaction of cyclohexene·NO_2 pairs is negligible. Since cyclohexene oxide and NO are the sole products, we conclude that the species photolyzed has the molecular formula $C_6H_{10}O_2N$. Its pair of intense absorptions at 1655 and 1644 cm^{-1} has ^{15}N and ^{18}O isotope shifts of 28 and 42 cm^{-1}, respectively, which are characteristic of N=O stretching fundamentals. Similarly, the strong 769/756-cm^{-1} doublet displays ^{15}N and ^{18}O frequency shifts corresponding to N–O stretching modes (in the case of the 769-cm^{-1} band, the isotope shifts are shared with the vibrational mode absorbing at 675 cm^{-1}; see Table I and the Discussion). Moreover, these two pairs of bands are very close to the nitrite group stretching absorptions of ethyl,[3] *cis*- and *trans*-2-butyl,[1,2] and isobutyl nitrite radicals[4] reported previously. Hence we propose that the spectrum of $C_6H_{10}O_2N$, Table I, originates from two stereoisomers of cyclohexyl nitrite radical.

We have been able to differentiate the infrared spectra of the two cyclohexyl nitrite radical forms experimentally by wavelength-selective photodissociation. A matrix cyclohexene/NO_2/Ar = 2.5/1/100 was irradiated at 590 nm (600 mW cm^{-2}) for 10 h in order to accumulate both stereoisomers of the cyclohexyl nitrite radical. Subsequent photolysis at 545 nm led to a decrease of all cyclohexyl nitrite radical bands, and Figure 3a shows the erosion of the ν(N=O) and ν(N—O) absorptions upon 30-min irradiation at 150 mW cm^{-2}. It can be seen from Figure 3b that when we continued photolysis at this wavelength for 6 h and then at 514/488 nm for 5 min (100 mW cm^{-2}), the 1655/769-cm^{-1} pair decreased about twice the amount of the 1644/756-cm^{-1} pair. This is opposite to the ratio observed upon irradiaion at 545 nm, Figure 3a. Relative absorbance losses for all cyclohexyl nitrite radical bands are presented in columns 4 and 5 of Table I. On the basis of the wavelength dependent absorbance depletion data the cyclohexyl nitrite radical absorptions could be grouped into two sets of bands. These are labeled I_1 and I_2 in Table I.

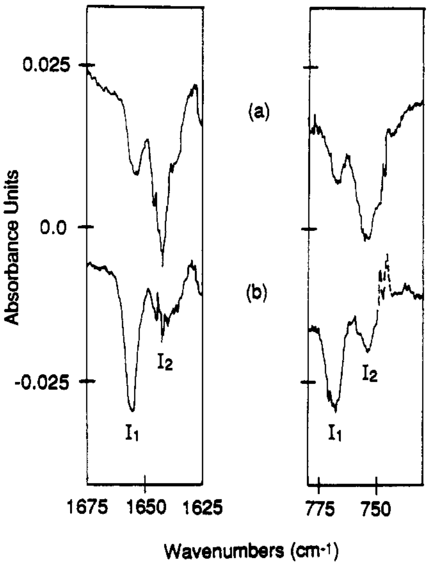

Figure 3. Wavelength selective photodissociation of cyclohexyl nitrite radical isomers: (a) absorption changes upon 30-min photolysis at 545 nm (150 mW cm^{-2}) following accumulation of cyclohexyl nitrite radical for 10 h at 590 nm (600 mW cm^{-2}) in a matrix cyclohexene/NO_2/Ar = 2.5/1/100; (b) loss of infrared absorption upon irradiation of the same matrix at 514/488 nm (100 mW cm^{-2}) for 5 min following prolonged 545-nm photolysis.

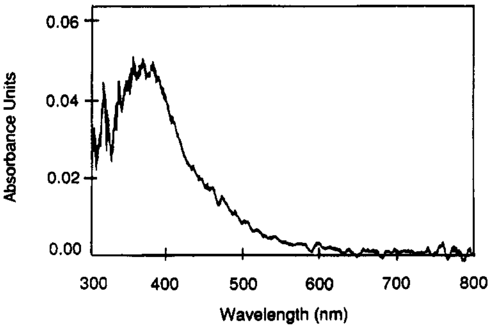

Figure 4. UV–visible spectrum of cyclohexyl nitrite radical (stereoisomer ratio I_1:I_2 ≈ 1). The spectrum constitutes the difference of spectra recorded before and after 10-min photolysis at 514/488 nm (100 mW cm^{-2}) of a matrix cyclohexene/NO_2/Ar = 2.5/1/100 following nitrite radical buildup by 6 h irradiation at 590 nm.

A visible spectrum of the electronic transition of cyclohexyl nitrite radical that is responsible for the observed photodissociation to cyclohexene oxide and NO is shown in Figure 4, and will be interpreted in a forthcoming paper.[10] It was obtained by taking

TABLE II: Infrared Spectrum Assigned to Cyclohexene Oxide in a Cyclohexene/NO_2/Ar (2.5/1/100) Matrix

frequency, cm^{-1}			
$C_6H_{10}{}^{16}O$[a]	$C_6H_{10}{}^{18}O$[b,d]	rel intensity[a]	A_3[c,d]
3007.5		0.3118	
2995.7		0.4624	
2985.5		0.2312	
2981.2		0.1855	
2949.8		(1.0000)	
2941.6		0.9732	
2934.5		0.4382	
2930.2		0.3790	
2925.1		0.3790	
2917.6		0.2635	
2895.0		0.1129	
2869.0		0.2259	
2850.0		0.1506	
1461.9	1461.9	0.2388	
1449.1		0.1208	
1444.2		0.1932	
1440.3		0.3219	
1428.5	1428.5	0.0966	0.097
1369.7	1369.7	0.0375	
1359.4	1359.4	0.0778	
1350.0	1350.0	0.0671	
1325.9	1325.9	0.0259	
1286.4		0.0349	
1267.8		0.1127	
1251.1		0.0482	
1194.2		0.0671	
1187.3		0.0831	0.083
1171.6		0.0591	
1150.0		0.0456	0.046
1086.9		0.0778	0.077
1058.4		0.0268	0.027
991.3		0.1234	0.123
968.1	958.0	0.4132	0.426
893.6	893.6	0.3783	
879.5	879.5	0.1718	
841.3	841.3	0.5796	
814.7	814.7	0.0509	
782.4	779.0	0.6091	
753.9		0.2656	
623.6		0.0321	
533.3	530.4	0.0912	

[a] Determined from a spectrum of cyclohexene oxide in argon (1/200) at 12 K (peak absorbances). [b] Frequency of peaks observed following 590-nm (400 mW cm^{-2}) irradiation of a cyclohexene/$N^{18}O_2$/Ar (2.5/1/100) matrix at 12 K for 5 h. [c] Relative intensity of peaks observed following 590-nm (400 mW cm^{-2}) irradiation of a cyclohexene/NO_2/Ar (2.5/1/100) matrix at 12 K for 3 h. [d] Frequency or relative intensity of bands that overlap cyclohexyl nitrite radical, cyclohexene, or N_xO_y absorptions is not given.

the difference of spectra recorded before and after 10-min photolysis at 514/488 nm (100 mW cm^{-2}) of a matrix cyclohexene/NO_2/Ar = 2.5/1/100 in which nitrite radical was first accumulated by prolonged irradiation at 590 nm.

Matrix temperature annealing experiments were conducted in order to find out whether the cyclohexyl nitrite radical isomers were thermally interconvertible. For this purpose, both Ar and Xe were used as host materials. After accumulation of I_1 and I_2 in matrices cyclohexene/NO_2/Ar and cyclohexene/NO_2/Xe = 2.5/1/100 by prolonged 590-nm photolysis, the matrix temperature was raised to 30 K. No thermal interconversion of the two stereoisomers was observed.

According to Figure 2, cyclohexene oxide and NO are produced by secondary photolysis of both cyclohexyl nitrite radical stereoisomers. To find out whether epoxide is produced by direct, single-photon photolysis of cyclohexene·NO_2 pairs in addition to secondary photolysis of cyclohexyl nitrite radical, product absorbance growth curves were measured at various photolysis wavelengths. Figure 5 shows the growth of cyclohexene oxide,

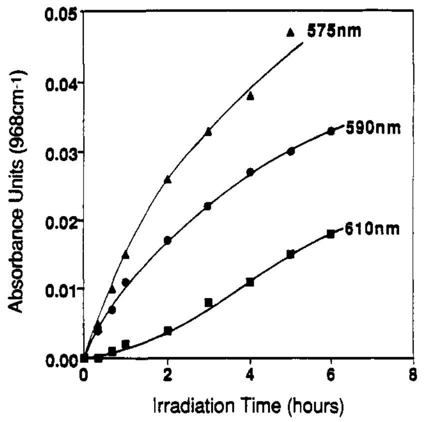

Figure 5. Absorbance growth behavior of cyclohexene oxide band at 968 cm^{-1} upon irradiation of matrices cyclohexene/NO_2/Ar = 2.5/1/100 at 610, 590, and 575 nm (500 mW cm^{-2}). Each curve has been obtained by starting with a new matrix.

TABLE III: Infrared Spectrum Assigned to Cyclopentyl Nitrite Radical Trapped in a Cyclopentene/NO_2/Ar (2.5/1/200) Matrix

frequency, cm^{-1}			rel intensity	
$C_5H_8{}^{16}ON^{16}O$	$C_5H_8{}^{18}ON^{18}O$	$C_5H_8O^{15}NO$	$A_{590\,nm}$[a]	$A_{514/488\,nm}$[b]
1645	1604	1615	(1.00)	(1.00)
787	777	777	*c*	0.58
750	735	744	0.59	0.58

[a] Relative intensity of peaks observed following 590-nm (400 mW cm^{-2}) irradiation of cyclopentene/NO_2/Ar (2.5/1/200) matrix at 12 K for 5 h. [b] Relative intensity loss of peaks assigned the trapped cyclopentyl nitrite radical following 514/488-nm (100 mW cm^{-2}) irradiation of cyclopentene/NO_2/Ar (2.5/1/200) matrix at 12 K for 15 min. [c] Band of trapped intermediate overlaps N_xO_y absorption.

as measured by the absorbance of the 968-cm^{-1} band, at three different photolysis wavelengths in matrices cyclohexene/NO_2/Ar = 2.5/1/100, namely, at 610, 590, and 575 nm (500 mW cm^{-2}). Each curve was determined by starting with a new matrix. Clearly, an induction period is observed at the 610-nm photolysis threshold energy, indicating that at this wavelength cyclohexene oxide is produced exclusively by secondary photolysis of cyclohexyl nitrite radical. However, the initial slope of the absorbance growth curves obtained at 590 and 575 nm exhibit a distinct nonzero slope at the start of photolysis. This implies that the epoxide and NO are concurrently produced by direct single-photon photolysis of cyclohexene·NO_2 reactant pairs at these shorter wavelengths.

(*B*) *Cyclopentene* + NO_2. As in the case of cyclohexene + NO_2, irradiation of matrices cyclopentene/NO_2/Ar at wavelengths shorter than 610 nm resulted in infrared spectral changes that indicated chemical reaction of C_5H_8·NO_2 pairs. For example, 30-min photolysis at 590 nm (400 mW cm^{-2}) of a matrix cyclopentene/NO_2/Ar = 2.5/1/200 led to product growth at 1645, 787, and 750 cm^{-1} (Table III) concurrent with loss of C_5H_8 and NO_2 infrared absorbance. Further photolysis at this wavelength gave rise to a number of additional product bands which are presented in Table IV, plus an absorption at 1872 cm^{-1} that originates from NO. Frequencies and intensities of the bands of Table IV agree with an authentic infrared matrix spectrum of cyclopentene oxide (M/A = 1/200, compare columns 3 and 4 of Table IV). As can be seen from Figure 6, subsequent irradiation with 514/488-nm light (100 mW cm^{-2}) for 15 min resulted in absorbance loss at 1645, 787, and 750 cm^{-1} and concurrent growth, at constant relative intensities, of all bands listed in Table IV. No product absorptions other than those given in Tables III and IV (and the 1872-cm^{-1} NO band) were observed upon irradiation of C_5H_8/NO_2/Ar matrices at any visible wavelength (610–458 nm).

Figure 6 shows that reaction of cyclopentene·NO_2 pairs upon brief photolysis with "blue-green" light is minimal compared to the amount of absorbance loss of the bands at 1645, 787, and 750 cm^{-1}. Hence our observation that cyclopentene oxide and NO are the only products of brief 514/488-nm photolysis implies that

---

(10) Fitzmaurice, D. J.; Frei, H. Manuscript to be submitted.

TABLE IV: Infrared Spectrum Assigned to Cyclopentene Oxide in a Cyclopentene/NO_2/Ar (2.5/1/100) Matrix

freq, cm^{-1}			
$C_5H_8{}^{16}O^a$	$C_5H_8{}^{18}O^{b,d}$	rel intensity^a	$A_5{}^{c,d}$
3042.2	3042.2	0.1516	
3028.4	3028.4	0.1444	
2981.4		0.2118	
2963.7	2963.7	0.3273	
2926.9		0.2094	
2910.8		0.1011	
2902.9		0.0674	
2878.4		0.0494	
2859.6		0.1721	
2838.2		0.0145	
1469.7	1465.3	0.0986	
1451.0		0.0507	
1442.3	1442.2	0.1726	
1396.3	1392.7	0.2466	0.28
1301.6	1300.0	0.2406	
1242.3		0.0568	0.07
1213.2	1205.5	0.1404	0.18
1092.3	1087.6	0.1623	0.20
1016.4	1015.7	0.0548	
938.2	932.4	0.3630	0.31
923.6	923.6	0.3685	0.39
843.3	831.4	(1.0000)	1.00
805.1	801.0	0.0548	0.08
656.3	652.7	0.0432	0.05
639.4	636.1	0.0856	

[a] Determined from a spectrum of cyclopentene oxide in argon (1/200) at 12 K. [b] Frequency of peaks observed following 590 nm (400 mW cm^{-2}) irradiation of a cyclopentene/$N^{18}O_2$/Ar (2.5/1/100) matrix at 12 K for 5 h. [c] Relative intensity of peaks observed following 590-nm (400 mW cm^{-2}) irradiation of a cyclopentene/NO_2/Ar (2.5/1/100) matrix at 12 K for 5 h. [d] Frequency or relative intensity of bands that overlap cyclopentyl nitrite radical, cyclopentene, or N_xO_y absorptions is not given.

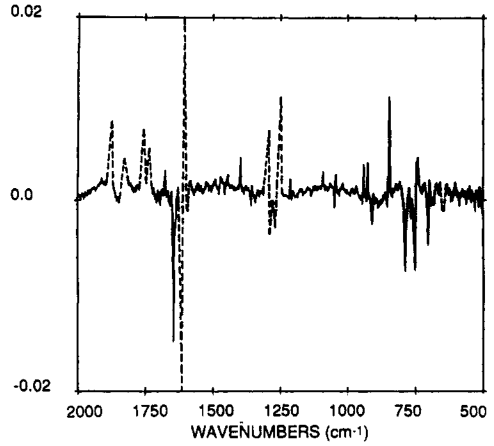

Figure 6. Infrared difference spectrum obtained upon 15-min 514/488-nm Ar ion laser photolysis (100 mW cm^{-2}) of a matrix cyclopentene/NO_2/Ar = 2.5/1/200 following prolonged irradiation at 590 nm.

the above three bands originate from a $C_5H_8O_2N$ species. The frequencies and the ^{15}N and ^{18}O isotope shifts of these three absorptions are given in Table III and clearly indicate the presence of a nitrite group. The 1645-cm^{-1} band is assigned to ν(N═O), while the N—O stretching mode contributes to the fundamentals absorbing at 787 and 750 cm^{-1}. We conclude that $C_5H_8O_2N$ is a cyclopentyl nitrite radical. In contrast to the cyclohexene + NO_2 reaction, which gave rise to two cycloalkyl nitrite radical isomers, in the case of cyclopentyl nitrite radical absorbance growth kinetics at all photolysis wavelengths was consistent with the presence of only one isomer (Table III, columns 4 and 5). Wavelength-dependent product growth kinetics similar to the cyclohexene + NO_2 case (Figure 5) showed that cyclopentene oxide and NO are produced by both single-photon photolysis of cyclopentene·NO_2 pairs and secondary photolysis of cyclopentyl nitrite radical.

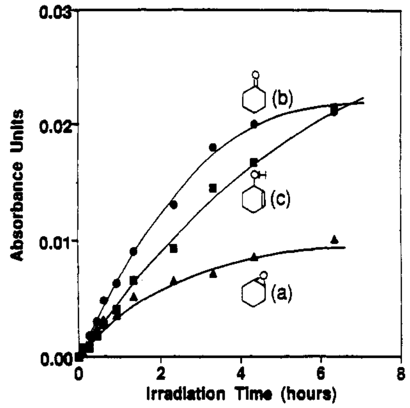

Figure 7. Absorbance growth kinetics upon irradiation of a matrix cyclohexene/NO_2/Ar = 2.5/1/200 at 355 nm (8 mW cm^{-2}): (a) cyclohexene oxide (968 cm^{-1}); (b) cyclohexanone (1723 cm^{-1}); (c) 2-cyclohexen-1-ol (1067 cm^{-1}).

TABLE V: Infrared Spectrum Assigned to Cyclohexanone in a Cyclohexene/NO_2/Ar (2.5/1/200) Matrix

freq,^{a} cm^{-1}	rel intensity^a	$A_6{}^{b,c}$	freq,^{a} cm^{-1}	rel intensity^a	$A_6{}^{b,c}$
2950	0.3252		1313	0.1382	
2870	0.1382		1220	0.1294	0.13
2860	0.0812		1122	0.1545	0.14
1730	(1.0000)	(1.00)	1050	0.0366	0.05
1723	0.4634	0.49	1020	0.0366	0.04
1450	0.1707		992	0.0162	
1430	0.0408		907	0.0570	
1350	0.0812		863	0.0529	
1340	0.1137		490	0.0446	

[a] Determined from a spectrum of cyclohexanone in argon (1/100) at 12 K. [b] Relative intensity of peaks observed following 355-nm (8.0 mW cm^{-2}) irradiation of a cyclohexene/NO_2/Ar (2.5/1/200) matrix at 12 K for 6 h. [c] Relative intensity of bands overlapping cyclohexene oxide, 2-cyclohexen-1-ol, or N_xO_y absorptions is not given.

3. Photolysis above the NO_2 Dissociation Limit. To find out whether the observed high product specificity of these ring epoxidations is a direct consequence of excitation of the alkene·NO_2 sustained collisional pairs below the 398-nm NO_2 dissociation limit, cyclohexene/NO_2/Ar and cyclopentene/NO_2/Ar matrices were photolyzed by 350-nm light. Experiments were performed with two laser sources, namely, the 351–364-nm lines of a CW Ar ion laser and the 355-nm output of a pulsed Nd:YAG laser. Results with the continuous and the pulsed laser were identical; hence we will limit our report to experiments with the more extensively used Nd:YAG source.

(*A*) *Cyclohexene + NO_2.* A matrix cyclohexene/NO_2/Ar = 2.5/1/200 was irradiated at 355 nm (8 mW cm^{-2}) for 6 h. While no absorption of cyclohexyl nitrite radical was observed, cyclohexene oxide and NO were readily detected. The growth behavior of the 968-cm^{-1} cyclohexene oxide band is shown in Figure 7a. Twelve additional absorptions grew in that were not observed at photolysis photon energies below the 398-nm NO_2 dissociation limit. Six of these, namely, at 1730, 1723, 1220, 1122, 1050, and 1020 cm^{-1} exhibited identical growth kinetics. Table V shows that frequencies and relative intensities of these bands agree with an authentic infrared matrix spectrum of cyclohexanone. The growth behavior of this new product is the same, within uncertainty limits, as that of cyclohexene oxide, as can be seen by comparing curves a and b of Figure 7. The remaining six bands at 1067, 1040, 958, 850, 804, and 670 cm^{-1} exhibit identical absorbance growth kinetics, which are distinctly different, however, from those of cyclohexene oxide or cyclohexanone. This can be readily seen by comparing curve c with curves a and b of Figure 7. It suggests that these absorptions originate from a single species, 2-cyclohexen-1-ol, according to the comparison with frequencies and intensities of an authentic infrared Ar matrix spectrum of this molecule, shown in Table VI. The 355-nm photolysis experiment was repeated with a much more dilute matrix, cyclohexene/

TABLE VI: Infrared Spectrum Assigned to 2-Cyclohexen-1-ol in a Cyclohexene/NO_2/Ar (2.5/1/200) Matrix

freq,[a] cm^{-1}	rel intensity[a]	$A_6^{b,c}$	freq,[a] cm^{-1}	rel intensity[a]	$A_6^{b,c}$
3655	0.1065		1040	(1.0000)	(1.00)
3032	0.3726		1034	0.2243	
2935	0.4753		1002	0.0608	
1440	0.1520		976	0.0760	
1404	0.1939		966	0.1331	
1395	0.2699		958	0.4905	0.51
1373	0.3118		916	0.3118	
1257	0.0798		895	0.2395	
1217	0.1103		880	0.3574	
1155	0.1939		850	0.0760	0.07
1090	0.1178		804	0.2852	0.28
1067	0.8935	0.95	730	0.5969	
1058	0.4487		718	0.1178	
1055	0.2852		670	0.1483	0.14
1050	0.2852		642	0.1179	
1047	0.2395				

[a] Determined from a spectrum of 2-cyclohexen-1-ol in argon at 12 K. [b] Relative intensity of peaks observed following 355-nm (8.0 mW cm^{-2}) irradiation of a cyclohexene/NO_2/Ar (2.5/1/200) matrix at 12 K for 6 h. [c] Relative intensity of bands overlapping cyclohexene oxide, cyclohexanone, or N_xO_y absorptions are not given.

TABLE VII: Infrared Spectrum Assigned to Cyclopentanone in a Cyclopentene/NO_2/Ar (2.5/1/200) Matrix

freq,[a] cm^{-1}	rel intensity[a]	$A_6^{b,c}$	freq,[a] cm^{-1}	rel intensity[a]	$A_6^{b,c}$
2979	0.3126		1269	0.0729	
2950	0.1051		1230	0.0381	0.04
2892	0.0782		1177	0.0443	0.05
1759	(1.0000)	(1.00)	1150	0.3968	0.40
1752	0.6665	0.56	1140	0.2951	0.27
1731	0.1619	0.17	956	0.1176	0.13
1725	0.1778	0.17	911	0.0127	
1470	0.0413		837	0.0984	
1457	0.0889		808	0.0222	
1423	0.0349	0.04	580	0.0443	
1412	0.2222	0.25	560	0.0443	
1283	0.0349				

[a] Determined from a spectrum of cyclopentanone in argon (1/100) at 12 K. [b] Relative intensity of peaks observed following 355-nm (8.0 mW cm^{-2}) irradiation of a cyclopentene/NO_2/Ar (2.5/1/200) matrix at 12 K for 6 h. [c] Relative intensity of bands overlapping cyclopentene oxide, 2-cyclopenten-1-ol, or N_xO_y absorptions is not given.

NO_2/Ar = 1/1/1000. The same products were observed, but the branching ratio of cyclohexenol to cyclohexene oxide increased by about a factor of 3 as indicated by the change of the absorbance growth ratio of the 1067-cm^{-1} alcohol absorption to the 968-cm^{-1} epoxide band from 0.5 at 2.5/1/200 to 1.5 at 1/1/1000 (both ratios measured after 6 h of 355-nm photolysis at 8 mW cm^{-2}). On the other hand, no significant dependence of the ratio of epoxide to cyclohexanone on concentration could be detected.

A series of photolysis experiments was conducted to learn more about the origin of these new products. Prolonged 355-nm irradiation of cyclohexene oxide suspended in solid Ar gave no reaction. This confirms that neither cyclohexanone nor cyclohexenol is produced by secondary photolysis of epoxide. Likewise, illumination of a matrix cyclohexanone/Ar resulted in no decomposition. We conclude that neither the ketone nor the alcohol observed upon 355-nm irradiation stems from secondary photolysis of final oxidation products. Nitric oxide does not absorb at this wavelength, and hence it cannot give rise to secondary photochemistry. Furthermore, cyclohexene oxide/NO_2/Ar and cyclohexanone/NO_2/Ar matrices were irradiated at 355 nm to find out whether photoinduced reaction of NO_2 with these products would yield 2-cyclohexen-1-ol. No reaction was observed.

Buildup of cyclohexyl nitrite radical through prolonged irradiation of a matrix cyclohexene/NO_2/Ar = 2.5/1/200 at 590 nm (9 h, 500 mW cm^{-2}), followed by brief photolysis at 355 nm (2 min, 8 mW cm^{-2}) resulted in a substantially larger ratio of cyclohexanone to cyclohexene oxide than measured upon photolysis at 355 nm under identical conditions, but without prior buildup of cyclohexyl nitrite radical. This is indicated by comparison of the absorbance growth ratio of the 1122-cm^{-1} cyclohexanone and the 991-cm^{-1} epoxide bands in the two experiments. The observed ratio is ≥10 upon 2-min irradiation at 355 nm if nitrite radical was first built up, and 0.2 for 2-min 355-nm photolysis in the case of no prior accumulation of radical. The implication is that upon 355-nm photolysis of a matrix cyclohexene/NO_2/Ar, a substantial fraction of cyclohexanone, possibly even all of it, emerges from seconday photolysis of cyclohexyl nitrite radical. It is important to note that the lack of observation of cyclohexyl nitrite radical upon 355-nm irradiation of cyclohexene/NO_2/Ar matrices and the apparent first order cyclohexanone growth do not contradict our conclusion that most, if not all, cyclohexanone originates from photodissociation of nitrite radicals. Photodissociation of cyclohexyl nitrite radical to cyclohexanone and NO at 355 nm may be efficient enough to result in radical steady-state concentration too low to be detected by infrared spectroscopy. Such a situation was encountered in the previously studied 2-butene + NO_2 system when irradiating at 514 nm, where we found a branching between epoxide and trapped nitrite radical around one, yet no nitrite radical could be observed.[1]

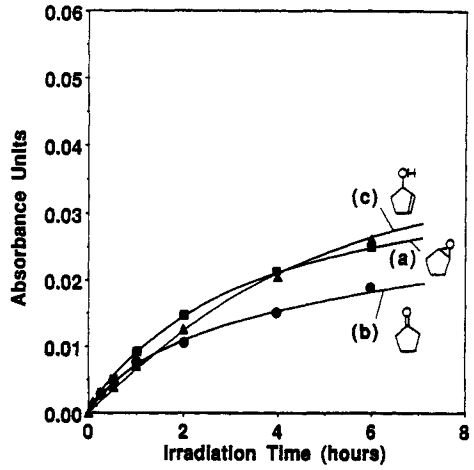

Figure 8. Absorbance growth behavior upon 355-nm (8 mW cm^{-2}) photolysis of a matrix cyclopentene/NO_2/Ar = 2.5/1/200: (a) cyclopentene oxide (938 cm^{-1}); (b) cyclopentanone (1150 cm^{-1}); (c) 2-cyclopenten-1-ol (1054 cm^{-1}).

(*B*) *Cyclopentene* + NO_2. In a 355-nm photolysis experiment with a matrix cyclopentene/NO_2/Ar = 2.5/1/200 (6 h at 8 mW cm^{-2}), we observed growth of cyclopentene oxide, NO, and 19 additional absorptions not encountered upon irradiation at photon energies below the NO_2 dissociation limit. Eleven of these additional absorptions behaved kinetically the same (1759, 1752, 1731, 1725, 1423, 1412, 1230, 1177, 1150, 1140, and 956 cm^{-1}), and their frequencies and relative intensities agreed well with an authentic Ar matrix spectrum of cyclopentanone, as shown in Table VII. While cyclopentanone and cyclopentene oxide had the same absorbance growth behavior according to curves a and b of Figure 8, it was significantly different from that of the remaining eight absorptions at 3605 (0.009), 1217, 1063 (0.004), 1054 (0.025), 1001 (0.003), 973 (0.009), 875 (0.007), and 671 cm^{-1} (0.009). Numbers in parentheses indicate absorbance growth after 6-h photolysis, and the ratio of these intensities were constant over the entire irradiation period (band at 1217 cm^{-1} overlaps with another species, hence the intensity is not given). Absorbance growth kinetics of the 1054-cm^{-1} band is shown in curve c of Figure 8. Although no authentic or literature infrared spectrum was available, observation of an OH stretching absorption (3605 cm^{-1}), the similarity with the IR spectrum of 2-cyclohexen-1-ol (Table VI), and mechanistic considerations presented in section IV suggest assignment to 2-cyclopenten-1-ol. No cyclopentyl nitrite radical was obtained upon 355-nm photolysis, presumably for the same reason as given for the cyclohexene + NO_2 case. By analogy, we assume that cyclopentanone originates mostly, possibly quanti-

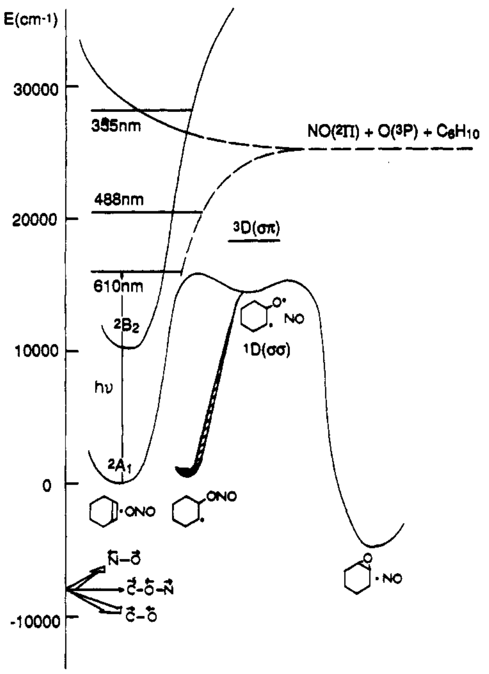

Figure 9. Potential energy diagram for the cyclohexene + NO_2 large-amplitude O atom transfer pathway. The corresponding energy diagram for the cyclopentene + NO_2 reaction is the same within the uncertainty of thermodynamic estimates.

tatively, from photodissociation of cyclopentyl nitrite radical.

IV. Discussion

We will first interpret the trapping of two cyclohexyl nitrite radical conformers and one cyclopentyl nitrite radical conformer in terms of the stereochemistry of the reaction paths of cyclohexene and cyclopentene oxidation, respectively. Then we will discuss the loss of product specificity upon excitation above the NO_2 dissociation limit.

1. Stereochemistry of Epoxidation Path. (A) Cyclohexene + NO_2. Figure 9 shows the energy profile of the O atom transfer path as suggested by the results of our previous studies of the reactions of *cis*- and *trans*-2-butene, and ethylene, with NO_2 in solid Ar.[1-3] This path leads to a transient oxirane biradical whose formation has been inferred from the stereochemical outcome of photooxidation of *cis*- and *trans*-2-butene by NO_2. Namely, it was found that the stereochemistry of the carbon skeleton of epoxide and alkyl nitrite radical are correlated, indicating that the two products have a common precursor whose conformation dictates the stereochemical outcome of the reaction. The observed high degree of stereochemical retention gave clear preference for oxirane biradical among possible candidates for precursor.[1,2] More recently, we have obtained further confirmation for O atom transfer as the initial step of long-wavelength visible light induced reaction of NO_2·hydrocarbon pairs in a matrix in our study of NO_2 + alkyne reactions.[11,12] By analogy, we propose that cyclohexene·NO_2 pairs vibronically excited by red or short-wavelength visible green or blue quanta undergo O atom transfer to form transient cyclohexene oxirane biradical. The branching between cyclohexyl nitrite radical and cyclohexene oxide + NO would be determined by the competition between combination of the oxirane biradical with a NO cage neighbor and closure of the ring.

The exothermicity $\Delta H° = -14.0$ kcal mol^{-1} of the reaction cyclohexene + $NO_2 \rightarrow$ cyclohexene oxide + NO used to construct the potential energy diagram (Figure 9) was calculated from known standard enthalpies of formation of the reactants. $\Delta H_f° = -28.5$ kcal mol^{-1} for cyclohexene oxide was determined by Benson's additivity rules for thermochemical properties.[13] $\Delta H°$ of cyclohexene + $NO_2 \rightarrow$ cyclohexyl nitrite radical was calculated as 1.6 kcal mol^{-1} on the basis of an estimate of $\Delta H_f° = 8.7$ kcal mol^{-1} for cyclohexyl nitrite radical derived as described in the Appendix of ref 1. In Figure 9, the endothermicity of the reaction cyclohexene + $NO_2 \rightarrow$ cyclohexene oxirane biradical + NO was taken as that of $C_2H_4 + NO_2 \rightarrow \dot{C}H_2CH_2\dot{O}$ ($^1D(\sigma\sigma)$) + NO, $\Delta H° = 41$ kcal mol^{-1}. This value was derived from ab initio calculations on $\dot{C}H_2CH_2\dot{O}$ by Fueno et al.[14] (the first orbital symbol in the electronic-state designation of the biradical indicates the orientation of the lone-electron p orbital on carbon with respect to the CCO plane, the second character the orientation of the singly occupied p orbital on the oxygen. σ designates in-plane, π indicates out-of-plane orientation).[15,16]

According to the most recent ab initio work on oxirane biradical,[14] the $^1D(\sigma\sigma)$ ground electronic state is the only state that can be reached with photons at wavelengths longer than 540 nm. The first excited state is predicted 12 kcal above the $^1D(\sigma\sigma)$ state ($^3D(\sigma\pi)$, Figure 9). Apart from this energy requirement, the high degree of stereochemical retention in both the epoxide and trapped nitrite radical in the case of *cis*- and *trans*-2-butene + NO_2 suggests that oxirane biradical is directly formed in the $^1D(\sigma\sigma)$ ground state.[1,2] In this biradical state, the singly occupied C and O p orbitals are in the CCO plane, and the state lies on the ground electronic surface of the epoxide. Therefore, ring closure is expected to be very fast, consistent with lack of internal rotation about the biradical C–C bond (thus preservation of stereochemistry) and the fact that ring closure can compete with activationless cage combination with NO. Moreover, if cyclohexene (or cyclopentene) oxirane biradical is forced initially into a triplet excited state by reaction of O(^{3}P) with the alkene, a completely different product, namely, an alcohol, is formed (see section IV.2).

Chemical trapping of transient cyclohexene oxirane biradical by reaction with a NO cage neighbor to form cyclohexyl nitrite radical in two distinct conformations furnishes insight into the stereochemistry of the reaction path that cannot be deduced from the structure of the final oxidation product. Cyclohexene oxide has a half-chair conformation[17] as does cyclohexene,[18] and hence comparison of reactant and product stereochemistry does not reveal which of the possible diastereomeric O atom transfer paths are pursued. The two nitrite radical isomers I_1 and I_2 could differ, in principle, with respect to the conformation about the N–O bond or the C–O bond or with regard to the stereochemistry of the hexyl ring.

The N=O stretching absorptions of the two cyclohexyl nitrite radical isomers at 1655 and 1644 cm^{-1} are close to the ν(N=O) bands of closed-shell alkyl nitrites with trans conformation about the N–O bond. For example, *trans*-$CH_3ON{=}O$ isolated in solid Ar absorbs at 1655 cm^{-1},[19] and *trans*-cyclohexyl nitrite (gas phase) at 1664 cm^{-1}.[20] Corresponding NO stretching absorptions for the cis forms (about the N–O bond) are reported at substantially lower frequencies, namely, at 1613 cm^{-1} (methyl nitrite)[19] and 1615 cm^{-1} (cyclohexyl nitrite).[20] The intense 769/756-cm^{-1} pair of the trapped cyclohexyl nitrite radical is also near the corresponding ν(N–O) absorption of closed-shell cyclohexyl nitrite at 775 cm^{-1}. This strongly suggests that both trapped cyclohexyl nitrite radical isomers have trans conformation about the N–O bond, as was previously observed for 2-butyl nitrite radical[1,2,4] and ethyl nitrite radical.[3] Therefore, the difference between I_1 and I_2 must be either in the conformation about the C–O bond or in the ring stereochemistry.

---

(11) Nakata, M.; Frei, H. Manuscript to be submitted.

(12) Harrison, J.; Frei, H. Manuscript in preparation.

(13) Benson, S. W. *Thermochemical Kinetics*; Wiley: New York, 1968.

(14) Fueno, T.; Takahara, Y.; Yamaguchi, K. *Proceedings of the Symposium on Molecular Structure*, Tokyo, 1986.

(15) Yamaguchi, Y.; Yabushita, S.; Fueno, T.; Kato, S.; Morokuma, K. *Chem. Phys. Lett.* **1980**, *70*, 27.

(16) Dupuis, M.; Wendoloski, J. J.; Takada, T.; Lester, W. A., Jr. *J. Chem. Phys.* **1982**, *76*, 481.

(17) Naumov, V. A.; Bezzubov, V. M. *J. Struct. Chem.* **1967**, *8*, 466.

(18) Anet, F. A. L. In *The Conformational Analysis of Cyclohexenes, Cyclohexadienes, and Related Hydroaromatic Compounds*; Rabideau, P., Ed.; VCH Publishers Inc.: New York, 1989; p 9.

(19) Gosh, P. N.; Gunthard, H. H. *Spectrochim. Acta* **1981**, *37A*, 1055.

(20) Tarte, P. *J. Chem. Phys.* **1952**, *20*, 1570.

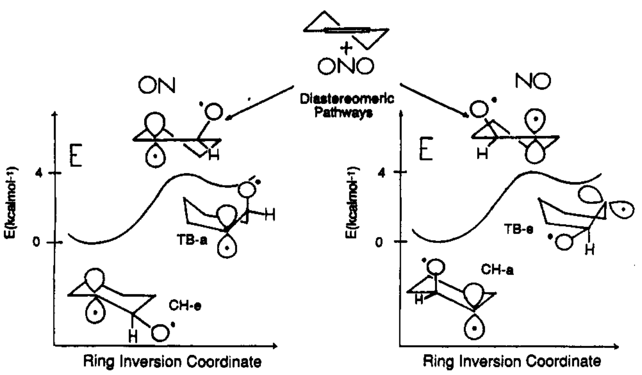

Figure 10. Stereochemistry of cyclohexene + NO_2 oxygen atom transfer path. Ring inversion potential of cyclohexene oxirane biradical is approximated by that of cyclohexyl radical (see text).[23]

It is unlikely that isomerism with respect to the C–O bond is responsible for trapping of two cyclohexyl nitrite radicals. First, infrared spectra of cyclohexyl nitrite molecules[20] do not indicate the presence of more than one conformer with respect to the C–O bond, as only isomerism with respect to the N–O bond is observed. Since the stereochemistry of the stable form of cyclohexyl radical is chair,[21,22] i.e., the same as for cyclohexane, and since the conformation of the nitrite group is also the same for cyclohexyl nitrite radical and molecule, it is difficult to see why the radical would exhibit rotational isomerism with respect to the C–O bond while the molecule does not. Second, no rotational isomerism about the C–O bond has been observed in any of the previously investigated acyclic alkyl nitrite radicals.[1-4] Particularly relevant is the comparison with *syn*-2-butyl nitrite radical,[2] since the stereochemistry in the vicinity of the nitrite group is virtually identical with that of cyclohexyl nitrite radical in its stable chair conformation. We therefore conclude that the structural difference between I_1 and I_2 is most probably associated with the stereochemistry of the hexyl ring, rather than the conformation about the C–O bond.

As shown in Figure 10, two diastereomeric paths are possible for O atom transfer to cyclohexene in its stable half-chair conformation (the only minimum on the ground-state potential surface).[18] These correspond to approach of the O atom on the two sides of the CC double bond. As illustrated in Figure 10, $sp^2 \rightarrow sp^3$ rehybridization of the attacked carbon results in bending of the olefinic H out of the plane of the former double bond. The branching between relaxation of the initial half-chair nuclear configuration of the ring to the twist-boat (TB) or chair (CH) minimum upon rehybridization may depend on the precise direction of O atom approach.[45] Therefore, as many as four diastereomeric oxirane biradicals could be formed, labeled CH-e, TB-a, CH-a, and TB-e in Figure 10 ("e" indicates equatorial, "a" axial position of the C–O bond, respectively). These would give rise to four spectrally distinguishable cyclohexyl nitrite radicals, as no change of the ring conformation is expected upon combination of the biradical with NO cage neighbor.[1-3] Yet only two diastereomeric cyclohexyl nitrite radicals are observed.

Three experimental findings suggest that I_1 is chemically trapped cyclohexene oxirane in the CH-e form and that I_2 is chemically trapped CH-a biradical. First, no thermal interconversion between I_1 and I_2 was observed even if the matrix temperature was raised as high as 30 K. Taking the experimental value for the activation energy of chair-to-chair interconversion of cyclohexyl radical (which is thought to proceed through twist-boat conformations) as a guide, we estimate the barrier for CH → TB isomerization of cyclohexyl nitrite radical to be around 4 kcal mol^{-1}.[21] Twist-boat cyclohexyl radical has not been observed thus far, but molecular mechanics calculations by Allinger[22] suggest that it is situated about 3.3 kcal mol^{-1} above the stable chair form. If we take this cyclohexyl radical potential as an approximation to that of cyclohexyl nitrite radical, NO-trapped oxirane biradicals TB-a and TB-e would have isomerization barriers to the corresponding chair forms of less than 1 kcal mol^{-1}. Thermal isomerization in a rare-gas solid involving a barrier around 1 kcal mol^{-1} occurs at 20 K in about 1 min.[25] Since no interconversion was observed even at 30 K, both I_1 and I_2 have most probably a stable chair conformation. Second, according to observed ^{18}O isotopic shifts of the two nitrite radicals in the 1200–800-cm^{-1} range (Table I), the C–O stretching mode of I_1 absorbs at 1050 cm^{-1}, while the ν(C–O) band of I_2 is at 960 cm^{-1}. According to infrared studies of 4-*tert*-butylcyclohexanol chair conformer,[26,27] the stretching mode of an axial C–O bond absorbs at 955 cm^{-1}, while the equatorial C–O stretch lies at 1062 cm^{-1} (at 1069 cm^{-1} in the case of unsubstituted cyclohexanol with an equatorial OH group). Although exceptions regarding this assignment of equatorial and axial C–O stretching absorptions have been reported,[28] a recent study of the infrared spectrum of *trans*-1,4-dimethoxycyclohexane tends to confirm it.[29] Hence the infrared spectroscopic evidence supports the assignment of CH-e nitrite radical to I_1 and NO-trapped CH-a to I_2.[30] Third, our observation that I_2 photoeliminates NO at green wavelengths with higher efficiency than I_1 is consistent with I_2 having an axial and I_1 having an equatorial oxygen. As can be seen from the structures in Figure 10, in the case of the CH-a form the lone electron p orbital on the carbon lies in the biradical CCO plane. The implication is that upon photoelimination of NO, the biradical has the proper alignment of oxygen and carbon p orbital to undergo ring closure. On the other hand, in the case of CH-e the C–O bond is perpendicular to the carbon p orbital, and hence substantial distortion of the hexyl ring is required for epoxide formation to occur. Hence I_1 is expected to exhibit a lower photodissociation yield than I_2, as observed. In terms of the stereochemistry of O atom transfer to cyclohexene, the implication of formation of cyclohexene oxirane biradicals CH-e and CH-a is that the transfer takes place along both diastereomeric paths, leading stereospecifically to one chair biradical along each path. The diastereomeric oxirane biradicals so formed are either trapped as cyclohexyl nitrite radicals by combination with NO cage neighbor or undergo ring closure to yield cyclohexene oxide. The lack of observation of twist-boat forms could be due to structural relaxation of the cyclohexene ring toward the stable chair form as the O atom approaches the CC double bond.[22,45] We cannot rule out the alternative possibility that initially trapped twist-boat cyclohexyl nitrite radicals thermally relax to stable chair forms on a time scale fast compared to Fourier transform infrared spectral measurements (minutes), although we do not consider it as likely.

(*B*) *Cyclopentene* + NO_2. By analogy with the cyclohexene + NO_2 reaction, O atom transfer from NO_2 to cyclopentene leads to transient cyclopentene oxirane biradical in the initial reaction step. The biradical is either chemically trapped as cyclopentyl nitrite radical by combining the NO cage neighbor, or it undergoes ring closure to form cyclopentene oxide in its single, envelope form. Thermodynamic estimates show that the energy profile of this reaction is essentially identical with that of cyclohexene + NO_2 displayed in Figure 9.

---

(21) Hori, Y.; Shimada, S.; Kashiwabara, H. *J. Phys. Chem.* **1986**, *90*, 3073. See also references therein.

(22) Imam, M. R.; Allinger, N. L. *J. Mol. Struct.* **1985**, *126*, 345.

(23) Taking the energy difference between the equatorial and axial conformer of cyclohexanol of 0.5 kcal mol^{-1} [24] as an upper limit for the energy difference between equatorial and axial chair (or twist-boat) oxirane biradical, we expect the relative energies of the biradical conformers to differ by no more than 15% from those of the corresponding cyclohexyl radical conformers.

(24) Wertz, D. H.; Allinger, N. L. *Tetrahedron* **1974**, *30*, 1579.

(25) Barnes, A. J. In *Matrix Isolation Spectroscopy*; Barnes, A. J., Ed.; Reidel: Dortrecht, 1981; p 531.

(26) Pickering, R. A.; Price, C. C. *J. Am. Chem. Soc.* **1958**, *80*, 4931.

(27) Hanack, M. *Conformational Theory*; Academic Press: New York, 1965; p 98, and references therein.

(28) Dyall, L. K.; Moore, R. G. *Aust. J. Chem.* **1968**, *21*, 2569.

(29) Zhizhin, G. N.; Sterin, Kh. E. In *Vibrational Spectra and Structure*; Durig, J. R., Ed.; Marcel Dekker: New York, 1981; Vol. 9, p 242.

(30) It should be noted that comparison of I_1 and I_2 infrared spectra with those of matrix isolated chair and twist-boat cyclohexane[31] does not furnish further evidence with regard to the chair vs twist-boat question as the vibrational spectra of the two C_6H_{12} forms do not exhibit characteristic bands.

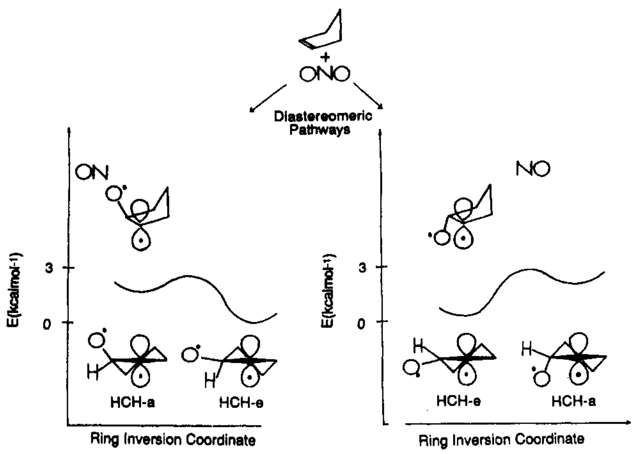

Figure 11. Stereochemistry of cyclopentene + NO_2 oxygen atom transfer path. Ring inversion potential of cyclopentene oxirane biradical is approximated by that of cyclopentyl radical (see text).

According to the nitrite group frequencies given in Table III, the conformation of cyclopentyl nitrite radical about the N–O bond is trans.[20] More importantly, only a single stereoisomer of cyclopentyl nitrite radical is observed, not two as in the case of the cyclohexene + NO_2 reaction. The reaction path diagram shown in Figure 11 may furnish an explanation. Two diastereomeric O atom transfer paths are possible if cyclopentene reacts in its stable envelope conformation.[33] These correspond to attack on one or the other side of the double bond. As in the case of cyclohexene + NO_2, we assume that the cyclopentene oxirane biradical ground-state potential can be approximated by that of the corresponding cycloalkyl radical. The stable conformation of cyclopentyl radical is half-chair (HCH), with a barrier to inversion between the two enantomeric forms of C_2 symmetry of 2.8 kcal mol^{-1}.[32] As can be seen from Figure 11 and from inspection of three-dimensional molecular models, one O atom transfer path would lead preferentially to HCH-a cyclopentene oxirane biradical (left), and the other to the HCH-e diastereomer (right). Observation of only one corresponding cyclopentyl nitrite radical stereoisomer is most probably due to thermal HCH-a → HCH-e pseudorotation of the ring after trapping of the two diastereomeric oxirane biradicals by NO, rather than diastereospecific O atom attack. The reason is that ring inversion of the reactant cyclopentene, which would destroy diastereospecificity, is too facile a process for one or the other path to dominate completely (E_a of 0.6 kcal mol^{-1}).[33] We conclude that the observed cyclopentyl nitrite radical has HCH-e conformation.

2. *Loss of Product Control upon Excitation above the NO_2 Dissociation Limit.* As can be seen from the energy diagram, Figure 9, cycloalkene·NO_2 collisional pairs excited at 355 nm to a $^2B_2$ predissociative level[34] have two competing reaction paths available in principle. The system could evolve along the large-amplitude O atom transfer coordinate to yield cycloalkene oxirane biradical + NO, i.e., the same path accessed by visible light excitation of nonpredissociative reactant vibronic levels. The second, new path would be crossing of NO_2 to its own repulsive surface (or direct coupling into the continuum of the $^2A_1$ ground electronic state), resulting in dissociation to $O(^3P)$ + $NO(^2\pi)$. Ground-state O atoms so formed could react thermally with cycloalkene. This second reaction path would also be available to cycloalkene·NO_2 pairs with unfavorable orientation for O atom transfer to occur through large-amplitude nuclear motion and to NO_2 separated from an alkene by one or several layers of Ar host atoms. Reaction along either path induced by 355-nm excitation could lead to products not observed upon irradiation of cycloalkene·NO_2 pairs with visible light as transient cycloalkene oxirane biradicals are produced with substantially higher excess internal energy at the shorter photolysis wavelength. Moreover, in the case of the NO_2 predissociation path the oxirane biradical would be initially forced into triplet excited state.

Loss of product specificity upon 355-nm excitation of cyclohexene + NO_2 and cyclopentene + NO_2 reactions is signaled by the appearance of two new products in each case, namely, a ketone and an alcohol. Cycloalkene oxide, the only final oxidation product upon visible light photolysis, is also formed. The fact that cyclohexanone (cyclopentanone) displays the same growth behavior as cyclohexene oxide (cyclopentene oxide) strongly suggests that this new product originates from the same reactant reservoir that is depleted upon photolysis with visible light, i.e., the reservoir of cycloalkene·NO_2 collisional pairs. We propose that upon 355-nm photolysis, epoxide and possibly some fraction of ketone are produced via ground-state $^1D(\sigma\sigma)$ oxirane biradical along the same large amplitude O atom transfer path operative upon initiation of the reaction with visible photons. This would be consistent with the fact that the cyclic ketones are 1,2-H shift products that can only originate from a singlet but not from a triplet oxirane biradical.[14,35,36] The branching of the biradical between 1,2-H migration to give ketone and ring closure to yield epoxide would be dictated by its excess internal energy and hence the energy of the photon that initiates the reaction. To the extent that ketone is produced along this path, the short photolysis wavelength required to observe it implies a higher barrier for 1,2-H migration of the biradical compared to that for ring closure. However, the data presented in Section III do not rule out the possibility that cycloalkenones are exclusively produced by 355-nm photodissociation of cycloalkyl nitrite radicals. The latter would be formed by NO trapping of transient oxirane biradical produced from cycloalkene·NO_2 collisional pairs along the large amplitude motion path. Since visible light photolysis of cyclohexyl and cyclopentyl nitrite radicals gives exclusively epoxide and no ketone, the cycloalkyl nitrite radicals apparently exhibit electronic state specific photochemistry. This will be discussed in a separate paper.[10]

The growth curves in Figures 7 and 8 show that both 2-cyclohexen-1-ol and 2-cyclopenten-1-ol originate from a reactant reservoir different from that of the collisional pairs. The only reactant that absorbs at 355 nm and whose reservoir increases relative to that of the pairs when decreasing the overall reactant to matrix gas ratio is isolated NO_2 (the branching ratio of epoxide (ketone) vs alcohol changes in favor of the alcohol when diluting the matrix). Therefore, we propose that cyclohexenol (cyclopentenol) is produced by dissociation of NO_2 to $O(^3P)$ and NO, followed by combination of oxygen atoms with cycloalkene. Although the $O(^3P)$ + cycloalkene step leads to triplet excited oxirane biradical initially, no conclusion can be drawn as to the biradical state in which subsequent 1,4-H migration to give cycloalkenol takes place.

Despite the loss of product specificity upon irradiation of cycloalkene/NO_2/Ar matrices above the NO_2 dissociation limit, the conclusion that the chemistry of cycloalkene·NO_2 collisional pairs proceeds preferentially along the same large-amplitude motion path already available at long photolysis wavelengths is intriguing. In fact, there are several recent reports of bimolecular reactions in cryogenic matrices and molecular beams that also point to preferred coupling of excited collisional pairs into large-amplitude atom transfer coordinates, rather than mere dissociation of reactants. Andrews and co-workers reported high efficiency of oxygen atom transfer in matrix isolated O_3·PH_3, O_3·P_4, O_3·PCl_3, O_3·AsH_3, O_3·SbH_3, and other ozone complexes upon irradiation with red light, but no reaction of isolated O_3 present in the same matrix.[37-40] This observation can be interpreted in terms of

---

(31) Offenbach, J. L.; Fredin, L.; Strauss, H. L. *J. Am. Chem. Soc.* **1981**, *103*, 1001.

(32) Sjöqvist, L.; Lindgren, M.; Lund, A. *Chem. Phys. Lett.* **1989**, *156*, 323.

(33) Burkert, U.; Allinger, N. L. *Molecular Mechanics*; American Chemical Society: Washington, D.C., 1982.

(34) Hsu, D. K.; Monts, D. L.; Zare, R. N. *Spectral Atlas of Nitrogen Dioxide*; Academic Press: New York, 1978.

(35) Lester, W. A., Jr.; Dupuis, M.; O'Donnell, T. J.; Olsen, A. J. *Frontiers in Chemistry*; Laidler, K. J., Ed.; Pergamon Press: New York, 1982; p 159.

(36) Schmoltner, A. M.; Chu, P. M.; Brudzynski, R. J.; Lee, Y. T. *J. Chem. Phys.* **1989**, *91*, 6926.

(37) Andrews, L. In ref 6, p 42.

(38) Withnall, R.; Andrews, L. *J. Phys. Chem.* **1987**, *91*, 784.

preferred coupling of predissociative $O_3(^1B_1)$, excited by red photons, into a large-amplitude O atom transfer coordinate that leads directly to products and that is not accessible to isolated O_3. UV light induced chemistry of acetylene·HI complexes in solid Kr by Abrash and Pimentel[41] constitute an extreme case in that photoexcitation promotes HI directly onto a dissociative surface. Yet there is evidence that even in this situation the reaction path does not involve formation of H atoms, but instead direct coupling of the excited HI·acetylene complex into C_2H_3 + I product states via a large amplitude I–H···C_2 coordinate. Access to this reaction path is attributed to the special T-shaped geometry of the complex formed by the reactants. The special chemistry of such precursor geometry limited bimolecular reactions has previously been recognized in molecular beam experiments by Wittig and co-workers[42] (e.g., photochemistry of CO_2·HBr complexes) and by Soep and collaborators[43,44] (e.g., $Hg\cdot H_2 \rightarrow HgH + H$). Of course, the product specificity in all cases of reactant excitation to dissociative or predissociative levels depends on reactant orientation. Coupling into large-amplitude reaction coordinates is possible only for complexes with proper geometry, while for all others reactant dissociation and subsequent free atom chemistry will prevail. The special benefit of excitation of collisional pairs below the lowest reactant dissociation threshold is that pairs with unfavorable geometry will not react at all and hence will not diminish the product specificity, only the yield. The fact that for all NO_2 + alkene systems studied so far[1-4] the depletion of the reservoir of alkene·NO_2 pairs upon prolonged photolysis with long-wavelength visible light is essentially complete suggests that reactant orientation is not critical for these reactions. This may be due to the large amplitudes of the highly vibrationally excited NO_2 that initiates the reaction.

V. Conclusions

Chemical trapping of transient cyclohexene and cyclopentene oxirane biradicals formed upon oxygen atom transfer from vibronically excited NO_2 to the CC double bond allowed us to map the detailed stereochemical path of cycloalkene oxidation for the first time. Observation of two diastereomeric cyclohexyl nitrite radicals with chair conformation in the case of cyclohexene is interpreted in terms of O atom transfer along two diastereomeric paths. These are not apparent from the stereochemistry of the final oxidation product. In contrast, a single cyclopentyl nitrite radical conformer is trapped, presumably because of much higher flexibility of the cyclopentyl system compared to the hexyl ring, allowing thermal pseudorotation of the trapped nitrite radical in the 12 K rare-gas solid.

The comparison of photochemistry initiated in cycloalkene/NO_2/Ar matrices with photons below and above the NO_2 dissociation threshold highlights the special chemistry of sustained collisional pairs in a matrix and points to the benefit, in terms of product control, of the use of long-wavelength photons to induce reaction. We find a single final oxidation product, cycloalkene oxide, at photon energies below the reactant dissociation limit where chemistry is restricted to the large-amplitude O atom transfer path. Product control is lost at photolysis photon energies above the NO_2 dissociation limit because predissociation becomes accessible, leading to formation of $O(^3P)$ and subsequently to free atom chemistry with alkene. Moreover, transient oxirane biradical produced upon 355-nm excitation along the large-amplitude reaction path emerges with substantially larger excess internal energy, which may open up reaction paths (1,2-H migration) not accessible at long photolysis wavelengths. Nevertheless, it is interesting that there remains a substantial propensity for cycloalkene·NO_2 sustained collisional pairs to couple into the large-amplitude O atom transfer path even above the NO_2 dissociation limit, apparently producing a singlet oxirane biradical as in the case of photolysis at wavelengths longer than 398 nm. Our finding that different oxidation products result from NO_2 predissociation (cycloalkenol) and large-amplitude reaction path (epoxide and ketone) allows us to monitor the branching between the two reaction channels. Since the two product paths reflect chemistry involving transient triplet and singlet oxirane biradical, respectively, it furnishes an opportunity to explore triplet and singlet alkene oxirane biradical reactivity in one and the same environment.

Acknowledgment. This work was supported by the Director, Office of Energy Research, Office of Basic Energy Sciences, Chemical Sciences Division of the U.S. Department of Energy under Contract No. DE-AC03-76SF00098.

Registry No. NO_2, 10102-44-0; $C_6H_{10}ONO$, 132128-64-4; $C_6H_{10}{}^{18}ON^{18}O$, 132128-65-5; $C_6H_{10}O^{15}NO$, 132128-66-6; $C_6H_{18}{}^{18}O$, 84279-02-7; C_5H_8ONO, 132128-67-7; $C_5H_8{}^{18}ON^{18}O$, 132128-68-8; $C_5H_8O^{15}NO$, 132128-69-9; $C_5H_8{}^{18}O$, 132128-70-2; cyclohexene, 110-83-8; cyclopentene, 142-29-0; 2-cyclopentenol, 3212-60-0; cyclopentene oxide, 285-67-6; cyclopentanone, 120-92-3; cyclohexene oxide, 286-20-4; cyclohexanone, 108-94-1; 2-cyclohexen-1-ol, 822-67-3.

---

(39) Moores, B. W.; Andrews, L. *J. Phys. Chem.* **1989**, *93*, 1902.

(40) Andrews, L.; Moores, B. W.; Fonda, K. K. *Inorg. Chem.* **1989**, *28*, 290.

(41) Abrash, S. A.; Pimentel, G. C. *J. Phys. Chem.* **1989**, *93*, 5828, 5834.

(42) Wittig, C.; Sharpe, S.; Beaudet, R. A. *Acc. Chem. Res.* **1988**, *21*, 341.

(43) Jouvet, C.; Boivineau, M.; Duval, M. C.; Soep, B. *J. Phys. Chem.* **1987**, *91*, 5416, and references therein.

(44) Breckenridge, W. H.; Jouvet, C.; Soep, B. *J. Chem. Phys.* **1986**, *84*, 1443.

(45) In earlier work on the steric course of radical attack on substituted cyclohexenes (e.g.: Huyser, E. S.; Jeffrey, J. R. *Tetrahedron* **1965**, *21*, 3083) partial stereospecificity observed upon approach of the double bond from the two sides has been interpreted, in part, by formation of TB-a and CH-a along paths corresponding to the left and right path in Figure 10, respectively. Although transient formation of twist-boat conformers would be consistent with experimental data, no evidence for the intermediacy of TB forms has been presented to our knowledge. Only stable CH conformers were observed, and the stereochemical course of the reactions can also be rationalized without assuming transient formation of unstable TB conformers.